

New Limits for Existence of Transverse Zero Sound in Fermi Liquid ^3He

M. D. Nguyen,^{*} D. Park, J. W. Scott, N. Zhelev, and W. P. Halperin[†]

Department of Physics and Astronomy,

Northwestern University

Evanston, IL 60208, USA

(Dated: October 15, 2024)

Abstract

Landau predicted that transverse sound propagates in a Fermi liquid with sufficiently strong Fermi liquid interactions, unlike a classical fluid which cannot support shear oscillations. Previous attempts to observe this unique collective mode yielded inconclusive results due to contributions from single particle excitations. Here, we have microfabricated acoustic cavities with a micron scale path length that is suitable for direct detection of this sound mode. The interference fringes of these acoustic Fabry-Pérot cavities can be used to determine both the real and imaginary parts of the acoustic impedance. We report a null-result in this search as no clear interference fringe has been observed in the Fermi liquid, indicating the attenuation of TZS is likely above 2000 cm^{-1} . We provide theoretical justification for why the sound mode may yet exist but not being directly detectable due to high attenuation.

INTRODUCTION

The Fermi liquid model, first proposed by Landau [3] and expanded later by many others, lies at the foundation of theoretical condensed matter physics and our understanding of the Fermi liquid state. Nearly all the central predictions of Landau's model have been verified, including the existence of longitudinal zero sound in liquid ^3He [4]. Landau also predicted the existence of another propagating sound mode called transverse zero sound (TZS), where the polarization of the wave is perpendicular to the wavevector (Fig. 1a). Measurements by Roach *et al.* [2] were initially believed to demonstrate the existence of TZS in ^3He but were later shown by Flowers *et al.* [1] to be the result of an incoherent quasiparticle excitation.

In the superfluid state, it was originally expected that transverse sound would be even harder to detect as the number of unpaired quasiparticles reduces with temperature. However, it was shown by Moores and Sauls that a new effect contributes to the stress tensor and is, in fact, much stronger than in the Fermi liquid case [5]. At frequencies above the imaginary squashing mode (ISQ) off-resonant coupling to this collective mode of the order parameter, drive current fluctuations leading to a strongly propagating TZS mode and the acoustic Faraday effect, demonstrated by Lee *et al.* [6]. Superfluid ^3He thus remains the only fluid where transverse sound waves have been observed. However, in the present work we revisit the normal Fermi liquid state to search for the last unverified prediction of Landau.

In a Fermi liquid, the shape of the Fermi surface governs the quasi-particle excitation energies and interactions between particles leading to changes in the quasi-particle distribution function, $n_{\mathbf{k}}$. Landau showed that the Fermi liquid interactions can be modeled as distortions of the Fermi surface in momentum space, as seen in Fig. 1(a). The Fermi surface can be thought of as a vibrating membrane and the interactions can be projected onto different angular momentum channels for corresponding distortions of the Fermi surface.

The dynamics of wave propagation in a Fermi liquid are governed by the Landau-Boltzmann kinetic equation [7]

$$i \left(v_F \hat{\mathbf{k}} \cdot \mathbf{q} - \omega \right) \Phi_{\hat{\mathbf{k}}} + i v_F \hat{\mathbf{k}} \cdot \mathbf{q} \int \frac{d\Omega_{\mathbf{k}'}}{4\pi} \mathbb{F}(\hat{\mathbf{k}} \cdot \hat{\mathbf{k}}') \Phi_{\hat{\mathbf{k}}'} = \delta I_{\hat{\mathbf{k}}}, \quad (1)$$

where v_F is the Fermi velocity, \mathbf{q} and ω are the wave-vector and the frequency of sound, $\Phi_{\hat{\mathbf{k}}}$ encodes the variation of the Fermi surface, where $\mathbb{F}(\hat{\mathbf{k}} \cdot \hat{\mathbf{k}}')$ are the Fermi liquid interactions between quasiparticles with momentum \mathbf{k} and \mathbf{k}' , and $\delta I_{\hat{\mathbf{k}}}$ is the linearized collision integral

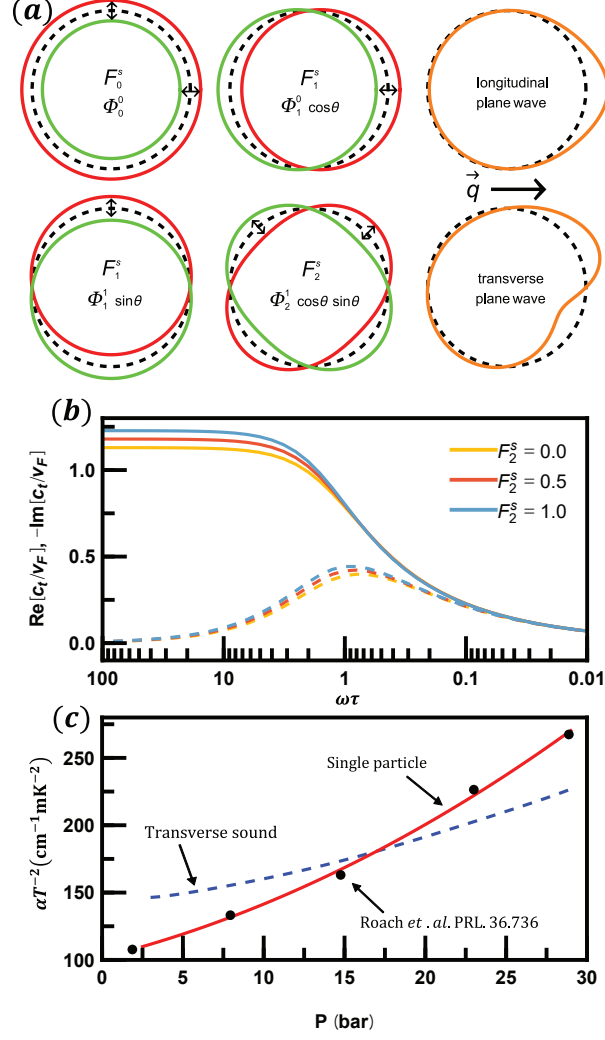


FIG. 1. (a) Oscillations of the Fermi surface for various l -channels and sound modes for rightward moving plane wave solution to Eq. 1 at $T = 0$. (b) Real (solid lines) and imaginary (dashed lines) of the transverse phase velocity in units of Fermi velocity as a function of $\omega\tau$ for various values of F_2^s at 22 bar. Solid lines and dashed lines stand for the real and imaginary speeds of transverse sound, respectively. (c) Comparison between theoretical model of Flowers *et al.* [1] with the data from Roach *et al.* [2] showing the pressure dependence of the observed attenuation is consistent with only the single particle contribution, indicating they did not observe transverse sound propagation.

for binary quasiparticle collisions. The Fermi liquid interactions can be projected in different angular momentum channels for spin-symmetric and spin anti-symmetric interactions. Only symmetric interactions are relevant for sound propagation. The strength of each l -channel is given by the Fermi liquid parameters F_l^s (s denoting spin symmetric).

The interplay between the collision and the Fermi liquid interaction terms in Eq. (1) determines the type of sound that propagates. At temperatures close to the Fermi temperature T_F , binary collisions dominate and sound is a classical hydrodynamic wave called first sound. In this hydrodynamic regime, the quasiparticle collision rate, $1/\tau$, is much higher than the frequency of sound so $\omega\tau \ll 1$. At temperatures $T \ll T_F$, the collision rate is low so collisions between particles are no longer sufficient to restore oscillations to equilibrium. Instead, the Fermi liquid interaction dominates and the sound mode is collision-less, called zero sound where $\omega\tau \gg 1$. Landau predicted that for sufficiently strong values of F_l^s , not only longitudinal zero sound, but also transverse zero sound, can exist.

While any positive, non-zero value of F_1^s leads to transverse current fluctuations, a transverse wave will only propagate if $\text{Re}[c_t/v_F] > 1$, where c_t is the transverse phase velocity. In the case where $\text{Re}[c_t]$ is equal to or just below v_F , resonant scattering between the wave and free quasiparticles can occur causing significant attenuation of the wave, a phenomenon called Landau damping [8]. This imposes a condition on the Fermi liquid parameters [9, 10]

$$\frac{F_1^s}{3} + \frac{F_2^s}{1 + F_2^s/5} > 2. \quad (2)$$

The interactions in liquid ^3He are rather strong, with F_1^s reaching ~ 15 at 34 bar meaning the interaction energy of this channel is 15 times the kinetic energy of a quasiparticle at the Fermi surface [11]. It is indeed remarkable that Fermi liquid theory accurately describes ^3He even when interaction strengths are far from a free Fermi gas. The condition of Eq. (2) is satisfied by liquid ^3He at almost all pressures and therefore TZS is expected to propagate.

Roach *et al.* measured the transverse acoustic impedance of ^3He , Z_H , as a function of temperature from the hydrodynamic regime (~ 100 mK) into the zero sound regime (~ 2 mK) [2], showing features that were thought to be consistent with a crossover from hydrodynamic to zero sound, similar to the shape in Fig. 1(b). In a classical medium, the ratio of the real part of the impedance to the density, $\text{Re}[Z]/\rho$, is equal to the speed of sound (for a given mode) so measurements of impedance are equivalent to measuring the speed of sound. In the case of TZS, this is no longer the case since there is a substantial

branching ratio into single quasiparticle excitations. The full expression for the acoustic impedance in the degenerate Fermi liquid ^3He will be published separately. It was shown that the incoherent quasiparticle excitation was responsible for the bulk of the impedance signal in the Roach *et al.* results [1], displayed in Fig. 1 (c).

To distinguish between TZS and an incoherent quasiparticle excitation, an interference experiment must be performed. Acoustic Fabry-Pérot interferometers have been used extensively to study TZS in the superfluid state including the discovery of the acoustic Faraday effect [6] as well as the observation of a new Cooper pair state [12]. In these experiments, a cavity is formed between a piezoelectric transducer and a reflecting plate shown in an inset in Fig 2(a). Depending upon the speed of sound and path length D , the reflected signal will destructively or constructively interfere with the transducer creating interference fringes. TZS can propagate with much lower attenuation in the superfluid state so cavities on the scale of $\sim 30 \mu\text{m}$ were used. Since the attenuation in the Fermi liquid state is expected to be substantial, $\mathcal{O}(1000 \text{ cm}^{-1})$ at 2 mK [13], the cavity for this experiment must be made smaller.

To ensure high parallelism between the two surfaces for a well-defined path length, we fabricated a $5.2 \mu\text{m}$ cavity out of a silicon-on-insulator (SOI) substrate (Fig 2a). SOI wafers have 3 layers, a device layer of silicon (Si) (typically micron scale), a buried oxide (BOX) layer of SiO_2 (typically $\leq 1 \mu\text{m}$), and finally a handle layer that is several hundred μm thick. The reflecting plate for our cavity is the Si handle layer while the spacer features are made of the BOX layer and device layer. The SOI wafer was chosen such that the device layer forms the bulk of the cavity spacing ($5 \mu\text{m}$) while the BOX layer adds 200 nm yielding a path length of $5.2 \mu\text{m}$. The fabrication out of an SOI wafer instead of simply silicon is to ensure a smooth reflecting surface. The dry-etching (Bosch) process of Si would lead to a very rough surface, not suitable for acoustic cavities. The BOX layer of the SOI wafer protects the handle layer's surface during the dry etching of the device layer. The BOX can be wet etched with hydrofluoric acid after the dry etch process, revealing the pristine handle layer. The transducer is an AC-cut (generating the transverse, thickness shear mode) quartz transducer with gold electrodes on the backside (non-cavity side). The fundamental frequency is 4.94 MHz and the transducer was mainly operated at the 21st (103.9 MHz) and 29th harmonics (143.7 MHz).

It is typical to characterize cavities in terms of their free spectral range (FSR), where

FSR = $\frac{2D}{c(P,T)}$ (the inverse of the round trip time). However, in acoustic systems where the wave is driven by a resonant transducer, frequency cannot be swept continuously (since the transducers response will only be large at discrete harmonics). On the other hand, the speed of sound can be easily modified by changing pressure thereby producing interference fringes like the ones shown in Fig 2(b) and (c). So it is more useful to work in terms of the free velocity range (FVR), where the FVR is given by $\Delta c(P,T) = \frac{2D}{f}$ (the difference in the speed of sound from one interference maximum to the next). In addition to the FVR (which encodes the variation in the speed of sound), the imaginary part of the acoustic impedance can also be inferred from this data. The amplitude of the interference pattern is proportional to the attenuation coefficient, α . An absolute measure of α can be extracted from this amplitude if it is compared with a signal of known attenuation.

Observing an interference pattern with a FVR consistent with TZS velocity in the Fermi liquid state would be direct evidence of a propagating sound mode which could not arise from the quasiparticle excitation. The direct observation of TZS cavity interference has several difficulties however. The biggest problem is the high attenuation of TZS in the FL state, shown in Fig. 3(a), which necessitates using small cavities to minimize loss. At 2 mK, α is approximately 500 cm^{-1} in the single relaxation time approximation [13]. In principle, reducing the cavity size from 30 microns to the low micron scale would make this very easily observed. However, cavities cannot be made too small since a shorter path length increases the FVR producing fewer interference fringes.

The drive frequency can be increased to compensate for the reduced fringes of a small cavity but the attenuation also has frequency dependence from two sources. In the relaxation time approximation, TZS has no frequency dependence with $\alpha \sim T^2$ (unlike in the hydrodynamic limit where $\alpha \sim \omega^2/T^2$ [7]). However if the sound energy $\hbar\omega$ is close to $k_B T$, then it can excite non-thermal quasiparticles which would contribute to the attenuation [7]. The crossover into what Landau calls the quantum limit of TZS begins when $\hbar\omega > 2\pi k_B T$. Far into the quantum regime where $\hbar\omega \gg 2\pi k_B T$, Landau predicts a simple quadratic frequency dependence of α . At 2 mK 100 MHz sound, $\frac{\hbar\omega}{2\pi k_B T} \sim 0.3$, is in the regime where some non-trivial frequency dependence is expected [14]. Finally if the full relaxation dynamics of the transport equation is considered, we expect additional frequency dependence [15].

Even with appropriate choice of cavity size and frequency, the number of interference fringes is ultimately controlled by the change in the speed of sound. In the superfluid state,

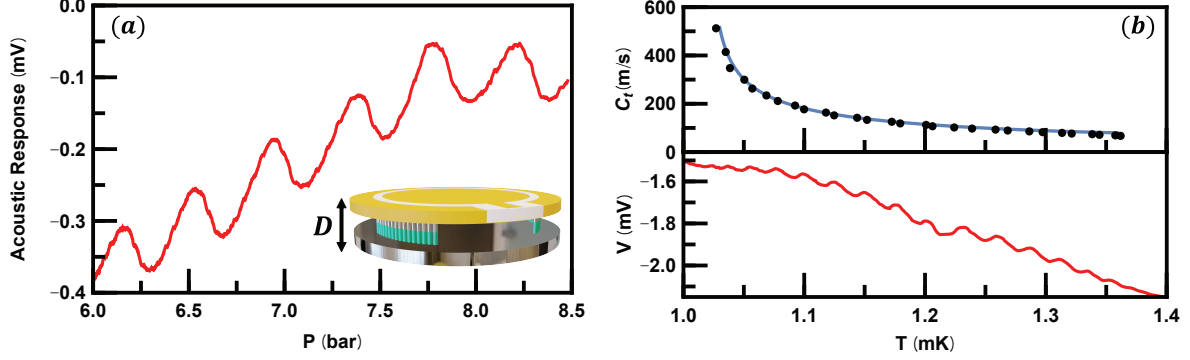


FIG. 2. (a) Interference fringes obtained during a pressure sweep in the superfluid state. Coupling between TZS and Higgs modes in the superfluid leads to a large change in the speed of sound. The pressure sweep was performed at $T/T_c \sim 0.45$ where the attenuation coefficient of TZS is roughly constant around 500 cm^{-1} [17]. The inset shows the acoustic cavity formed between a piezoelectric AC-cut quartz transducer (top, gold disk) and a microfabricated silicon reflecting plate (bottom disk), not to scale. (b) Interference fringes obtained during a temperature sweep at 10.5 bar and 103.9357 MHz in the superfluid state which can be used to calculate the speed of sound showing good agreement with the theory of Moores and Sauls [5] for a cavity size of $5.2 \text{ } \mu\text{m}$.

there is an off-resonant coupling between sound and the Higgs modes which greatly modifies the dispersion of sound [16]. The change in the sound velocity is significant leading to many interference maxima. Unlike in the superfluid, c_t in the Fermi liquid changes very little with pressure. The pressure dependence occurs separately in v_F and $\text{Re}[S_t]$, where $S_t = c_t/v_F$ is the reduced velocity. The Fermi velocity decreases from 59 m/s at 0 bar to 32 m/s at 34.39 bar. Unfortunately, c_t varies less with pressure than v_F since $\text{Re}[S_t]$ increases with pressure. Notwithstanding these difficulties, the number of interference fringes for a cavity of $5 \text{ } \mu\text{m}$ operated at 100 MHz should be well within the sensitivity range of the transducers used and it is expected that direct evidence for TZS or at least bounds on its attenuation can be determined.

NUMERICAL CALCULATION OF CAVITY INTERFERENCE

Flowers and Richardson[1, 18] considered an oscillating semi-infinite plate with two relaxation times to explain the high attenuation of TZS. These two relaxation times will

be discussed later based on the model of Kuorelahti *et al.*[19] who numerically solved the Landau-Boltzmann equation for a cavity. To predict the behavior of TZS in a $5.2 \mu\text{m}$ cavity with frequency of 103.9 MHz and 143.7 MHz, we used this model for the simulation shown in Figure 3. with $\xi = \tau_c/\tau_{viscous} = 0.35$.

Figure 3(b) shows the complex transverse impedance Z' with, and without, the reflecting plate at three different pressures. Above 5 mK, corresponding to the hydrodynamic regime, the transverse sound is diffuse and highly attenuated. Therefore, the impedance in the cavity becomes identical to that without the reflecting plate. However, the temperature enters the zero sound regime in the Fermi liquid below 5 mK. Because of the reduced attenuation, as shown in Fig.3 (a), the transverse sound propagates and the reflecting sound affects the oscillating plate. This causes the complex impedance in the cavity to deviate from the solid line shown in Fig.3 (b). The simulation results are compared to the experiments in Fig.3 (c), showing imaginary parts of the impedance from a pressure sweep and various temperature sweeps. At a fixed temperature of 2.3 mK, the speed of TZS is enhanced as the pressure increases, leading to the interference in the imaginary impedance Z'' . This is the expected amplitude and periodicity of interference in the cavity, based on a two relaxation time model[10]. To compare the numerical result with experiment data, this Z'' is converted into a frequency shift from the relations;

$$Z = Z' + iZ'' = \frac{1}{4}n\pi Z_q \Delta Q^{-1} + i \left(\frac{1}{2}n\pi Z_q \frac{\Delta f_0}{f_0} \right) \quad (3)$$

where n is n-th order in harmonics, Z_q is the impedance of quartz, Q is Q-factor and f_0 is the n-th harmonic frequency.

RESULTS

We first performed experiments in the superfluid (SF) state to characterize the quality of the cavities and calibrate α sensitivity. The figure of merit for how sensitive a cavity is to detecting TZS is amplitude attenuation factor for a round trip across the cavity, $\delta\mathcal{A} = e^{-\alpha 2D}$ (D is the cavity size). The amplitude of the interference fringes is proportional $\delta\mathcal{A}$. If the amplitude of interference can be determined for a known value of α , then it can be used to estimate the cavities detection sensitivity to highly attenuated signals. From past experiments, the smallest $\delta\mathcal{A}$ detected was ~ 0.03 [17]. There is not an exact mapping to TZS

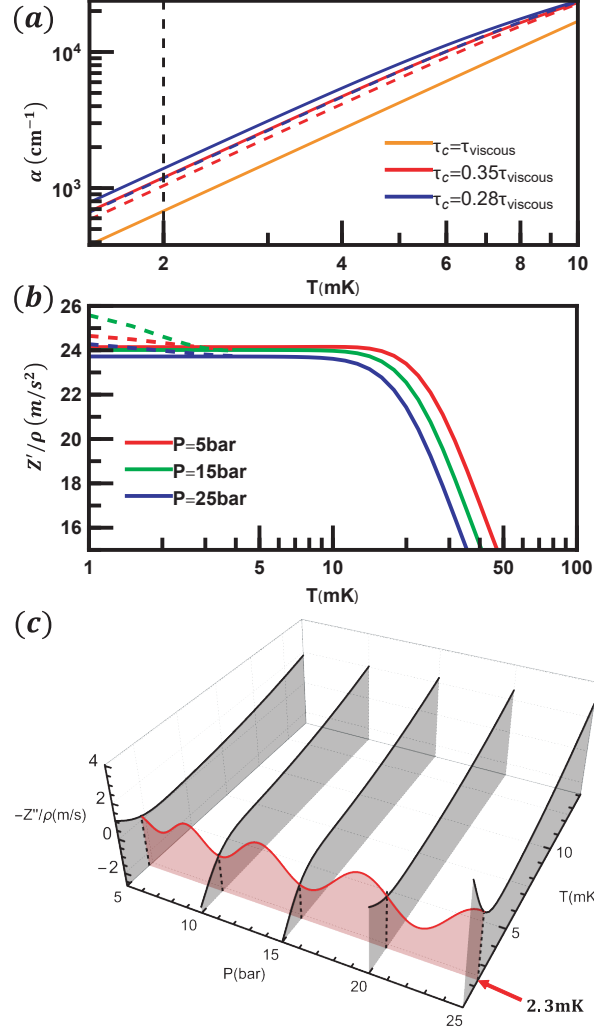


FIG. 3. (a) Attenuation coefficient, α , of TZS as a function of temperature, F_2^s , and relaxation time showing $\alpha \sim T^2$. All pressure sweeps we performed at the lowest temperature the Fermi liquid can exist, around 2 mK represented by the vertical dashed line. Note that F_2^s in the solid lines and dashed lines are 0 and 1, respectively. (b) Dashed lines show complex transverse impedance for a $5.2 \mu\text{m}$ cavity in the Fermi liquid state based on the theory of Kuorelahti *et al.*[19] at three different pressures (5, 15, and 25 bars) with the frequency of 103 MHz. For comparison, the solid lines obtained in the theory of Richardson[18] represent the case without the reflecting plate. Due to the reflecting plate, the complex impedance Z' in the zero-sound regime (below 5 mK) starts to deviate from the solid lines. (c) the imaginary part of the transverse impedance Z'' under a pressure sweep at 2.3 mK (red line) and temperature sweep at various fixed pressures (black lines). Except for $\xi = \tau_c/\tau_{\text{viscous}} = 0.35$, all parameters used in the simulation were tabulated in Ref [11]. Also, the diffusive boundary condition is applied in the simulation. The attenuation at 2.3 mK in the simulation is approximately 1000 cm^{-1} .

in the Fermi liquid since there is expected to be far fewer fringes making it harder to distinguish the interference pattern from the background shift in the impedance. Nonetheless, the amplitude of the interference fringes can still be a good metric for comparison.

Transverse zero sound (TZS) is rather well understood in the superfluid state both experimentally and theoretically. There is some disagreement between the two for the attenuation since the theory does not factor in surface Andreev bound states (SABS) that [17] contribute to attenuation. Without SABS, α is expected to decrease to close to 0 at $T = 0$ for $M_{2-} < \omega < 2\Delta$ (there is expected to be finite attenuation of sound even at $T=0$ from spontaneous emission due to vacuum fluctuations), where M_{2-} is the energy for the imaginary squashing mode in the B-phase. However, it was observed that α saturates around 400 to 500 cm^{-1} , independent of pressure. There is no observed decrease in α below $0.5 T_c$. This actually provides a good reference point for our experiments here. By cooling to around $0.5 T_c$ and performing a pressure sweep, one can obtain the approximate expected amplitude of the interference fringe for TZS propagating with 500 cm^{-1} of attenuation. This will allow us to put bounds upon α in the Fermi liquid (FL) state.

Both temperature and pressure sweeps are used to calibrate our cavities. A demagnetization cooling temperature sweep at 103.9357 MHz and 10.5 bar is shown in Fig. 2(b). The changing temperature tunes the superfluid gap Δ , the Tsuneto function, and the Higgs mode frequency. As the resonance with the Higgs is approached, the speed of sound sharply increases. The interference fringes can be used to calculate speed of sound and compared with the theoretical model of Moores and Sauls [5] (Fig. 2(bS)). This relatively good agreement indicates that the cavity support structure retains its integrity during cooldown.

After verifying the performance of the cavities in the SF state and establishing a reference for α , we performed a series of pressure sweeps in the FL state at temperatures just hovering above T_c of the SF. The attenuation of TZS in the FL state decreases as $\alpha \sim T^2$, as seen in Fig. 3, so its best to search for the interference at the lowest temperature where the FL state is stable.

Pressure sweeps at 21st(103.9 MHz) and 29th (143.7 MHz) harmonics of the transducer are shown in Fig 4. For Fig 4(a), the RF spectrometer was tuned to a single frequency (103.9352 MHz) while tracking the reflected signal from the transducer. The red and green curves show the expected amplitude and periodicity of the interference pattern for TZS with an attenuation coefficient of $\alpha = 500 \text{ cm}^{-1}$ and 2000 cm^{-1} , respectively. The amplitudes of

these curves were scaled from the result in the superfluid state for the known signal in this cavity for TZS with $\alpha \sim 500 \text{ cm}^{-1}$. It is evident that there are no interference fringes observed that are consistent with TZS.

For Fig 4(b), a network analyzer (VNA) was used to sweep across the full spectrum of the 29th harmonic around 143.7 MHz while performing the pressure sweep. The spectral line was then fit to a Lorentzian and the central frequency was extracted. The expected periodicity and amplitude of this pattern is obtained from the numerical simulation of the model from Kuorelahti *et al.* [19]. Note that the frequency shifts were derived from Eq. (3). Again, it is evident that there are no interference fringes with the correct FVR.

While it cannot be concluded that transverse sound does not propagate in the FL state, it can be said that the actual attenuation must be significantly higher than theoretically predicted within the relaxation time-approximation. At 2 mK, we conclude that the attenuation of sound is probably greater than 2000 cm^{-1} and likely to be the case at other pressures and frequencies. This is a marked extension of what has been reported in past studies [1, 2, 20] where the imaginary part of the acoustic impedance, Z'' , was found to be higher than predicted.

DISCUSSION

There is a reasonable theoretical basis for why the attenuation may be significantly higher than expected. The Landau-Boltzmann equation (Eq. 1) has a collision term that must be modeled. The simplest case is called the relaxation-time approximation where it is assumed fluctuations relax back to equilibrium exponentially with some time constant τ (i.e. δI is proportional to the disturbance, $\frac{\Phi_{\mathbf{k}}}{\tau}$). Lea *et al.* assumed this to be the case yielding an approximate attenuation of 500 cm^{-1} at 2 mK. You can generalize this assumption by allowing each l -channel fluctuation to relax at a separate rate. Usually this is truncated to some number of channels, such as was done by Flowers *et al.* [10] where they considered 2 relaxation times. The relaxation time of the collective part of the oscillation (sound), τ_c , is assumed to be different from the relaxation time obtained from viscosity measurements [21], τ_{viscous} , with a parameterization

$$\tau_c = \xi_2 \tau_{\text{viscous}}. \quad (4)$$

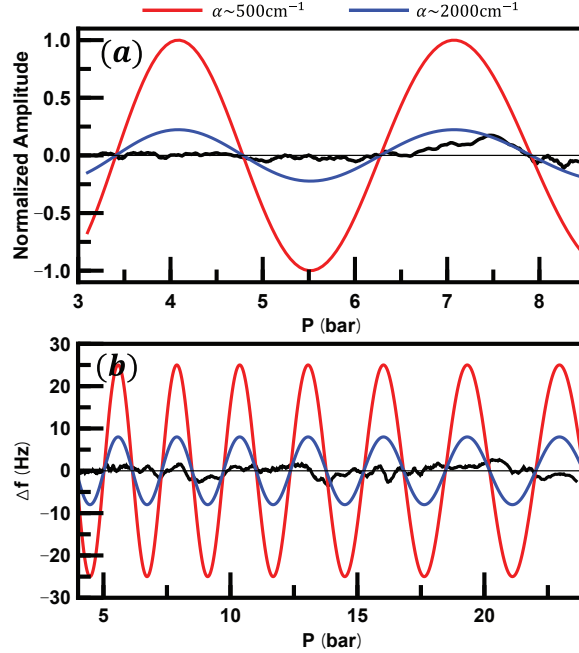


FIG. 4. Pressure sweep data in the Fermi liquid state around 2 mK compared with the expected interference pattern obtained from numerically solving the Landau-Boltzman equation in a $5.2 \mu\text{m}$ cavity. (a) Pressure sweep at a single fixed frequency using our CW spectrometer at fixed frequency, 103.9352 MHz.. The green curve shows the expected amplitude for TZS with an attenuation of $\alpha = 500 \text{ cm}^{-1}$ while the red curve shows the expected amplitude for $\alpha = 2000 \text{ cm}^{-1}$. (b) Pressure sweep while also sweeping the full resonance line of the 29^{th} around 143.7 MHz. The spectrum is fit to a Lorentzian and the central frequency is extracted. Both sweeps show no evidence of an interference pattern consistent with a propagating TZS mode. If TZS does propagate, the attenuation coefficient is likely $> 2000 \text{ cm}^{-1}$.

The quasiparticle relaxation time τ is taken to be the same as τ_c while the viscous relaxation time is taken to be mostly due to the relaxation of $l = 2$ channel [10, 18]. In other words, the quadrupolar fluctuations ($l = 2$) of the Fermi surface relax with a time constant $\tau_2 = \tau_{\text{viscous}} = \tau/\xi_2$.

Estimates have been made from various experiments with $\xi_2 = 0.35$ [22] or $\xi_2 = 0.28$ [23]. The smaller ξ_2 , the greater the attenuation of sound with $\xi_2 = 0.28$ yielding about 1300 cm^{-1} , as seen in Fig. 3. The two-relaxation time model indicates that for a given temperature, ^3He is at a lower value of $\omega\tau$ than naively expected in the one-relaxation time model. Consequently, the cavities are probing sound that is not as deep into the zero sound

regime as anticipated, leading to higher attenuation.

As seen from the multiple relaxation time model, the attenuation can vary greatly by allowing for complex relaxation dynamics. Furthermore, the value of F_2^s has a significant role in determining α . In fact, it is of similar order of magnitude as changing ξ_2 from 0.28 to 0.35, shown in Fig. 3. This might account for the considerable disagreement on the value of F_2^s reported from a number of experiments [11]. Additional contributions to the impedance (and correspondingly attenuation) result from consideration of vertex corrections to the quasiparticle propagator [15]. Shahzamanian and Yavary found that this introduces an explicit frequency dependence to the impedance. The conclusion we draw from our observations previous experiments and the various theoretical models is that the high attenuation of TZS in the Fermi liquid has prevented any direct detection of the mode from acoustic cavity interference.

This work was supported by NSF Division of Materials Research Grant No. DMR-2210112. We are grateful to J. A. Sauls, A. Vorontsov, J. A. Kuorelahti, and E. V. Thuneberg for useful discussion.

* mannguyen2019@u.northwestern.edu

† w-halperin@northwestern.edu

- [1] E. G. Flowers, R. W. Richardson, and S. J. Williamson, Phys. Rev. Lett. **37**, 309 (1976).
- [2] P. R. Roach and J. B. Ketterson, Phys. Rev. Lett. **36**, 736 (1976).
- [3] L. D. Landau, Sov. Phys. JETP **3**, 920 (1957).
- [4] W. R. Abel, A. C. Anderson, and J. C. Wheatley, Phys. Rev. Lett. **17**, 74 (1966).
- [5] G. F. Moores and J. A. Sauls, J. Low Temp. Phys. **91**, 13 (1993).
- [6] Y. Lee, T. M. Haard, W. P. Halperin, and J. A. Sauls, Nature **400**, 431 (1999).
- [7] L. D. Landau, Sov. Phys. JETP **5**, 101 (1957).
- [8] L. Landau, J. Phys. (USSR) **10**, 25 (1946).
- [9] I. A. Fomin, Sov. Phys. JETP **27** (1968).
- [10] E. G. Flowers and R. W. Richardson, Phys. Rev. B **17**, 1238 (1978).
- [11] W. P. Halperin and E. Varoquaux, in *Helium Three*, Modern Problems in Condensed Matter Sciences, Vol. 26, edited by W. P. Halperin and L. P. Pitaevskii (Elsevier, 1990) Chap. 7.

- [12] J. P. Davis, J. Pollanen, H. Choi, J. A. Sauls, and W. P. Halperin, *Nature Phys.* **4**, 571 (2008).
- [13] M. J. Lea, A. R. Birks, P. M. Lee, and E. R. Dobbs, *J. Phys. C* **6**, L226 (1973).
- [14] K. Matsumoto, T. Ikegami, and Y. Okuda, *Physica B: Condensed Matter* **194-196**, 743 (1994).
- [15] M. A. Shahzamanian and H. Yavary, *Int. J. Mod. Phys. B* **21**, 2979 (2007).
- [16] J. A. Sauls, *J. Low Temp. Phys.* **208**, 87 (2022).
- [17] J. P. Davis, J. Pollanen, H. Choi, J. A. Sauls, and W. P. Halperin, *Phys. Rev. Lett.* **101**, 085301 (2008).
- [18] R. W. Richardson, *Phys. Rev. B* **18**, 6122 (1978).
- [19] J. A. Kuorelahti, J. A. Tuorila, and E. V. Thuneberg, *Phys. Rev. B* **94**, 184103 (2016).
- [20] F. P. Milliken, R. W. Richardson, and S. J. Williamson, *J. Low Temp. Phys.* **45**, 409 (1981).
- [21] J. C. Wheatley, *Rev. Mod. Phys.* (1975).
- [22] D. T. Lawson, W. J. Gully, S. Goldstein, R. C. Richardson, and D. M. Lee, *Phys. Rev. Lett.* (1973).
- [23] P. Wölfle, *Phys. Rev. B* **14**, 89 (1976).